Analytica Chimica Acta xxx (2016) 1–10

Contents lists available at ScienceDirect

Analytica Chimica Acta

journal homepage: www.elsevier.com/locate/aca

Plasmon-enhanced fluorescence imaging with silicon-based silver chips for protein and nucleic acid assay

Bing Yuan [a, b, *, 1], Xiangxu Jiang [d, 1], Chu Yao [a, b], Meimei Bao [a, b], Jiaojiao Liu [a, b], Yujiang Dou [c], Yinze Xu [f], Yao He [d, ***], Kai Yang [a, b, **], Yuqiang Ma [a, b, e]

[a] College of Physics, Optoelectronics and Energy, Soochow University, Suzhou 215006, PR China
[b] Center for Soft Condensed Matter Physics and Interdisciplinary Research, Soochow University, Suzhou 215006, PR China
[c] School of Electronic and Information Engineering, Soochow University, Suzhou 215006, PR China
[d] Institute of Functional Nano and Soft Materials (FUNSOM), Jiangsu Key Laboratory for Carbon-Based Functional Materials and Devices, Soochow University, Suzhou 215123, PR China
[e] National Laboratory of Solid State Microstructures and Department of Physics, Nanjing University, Nanjing 210093, PR China
[f] School of Engineering, University of Guelph, Guelph N1G 2W1, Canada

HIGHLIGHTS

- A type of plasmonic Ag@Si chips composing of Si supported Ag film was fabricated.
- The chips show viable integration into fluorescent immunoassays for enhancement.
- The chips show up to 57 times enhancement at 800 nm in fluorescence protein assay.
- The chips show up to 4.1 times fluorescence enhancement for cell and tissue imaging.

GRAPHICAL ABSTRACT

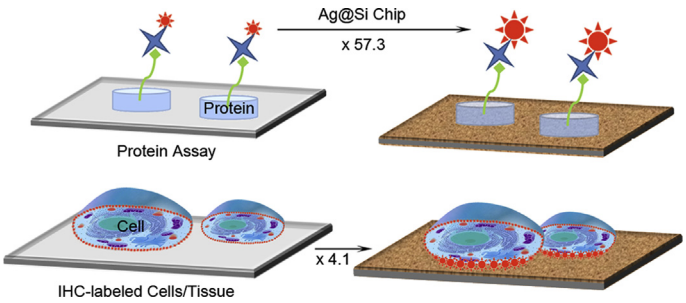

ARTICLE INFO

Article history:
Received 4 May 2016
Received in revised form
21 November 2016
Accepted 22 November 2016
Available online xxx

Keywords:
Surface-plasmon enhanced fluorescence
Silicon-supported silver-chip
Protein assay
Nucleic acid assay
Signal/background ratio

ABSTRACT

Metal-enhanced fluorescence shows great potential for improving the sensitivity of fluoroscopy, which has been widely used in protein and nucleic acid detection for biosensor and bioassay applications. In comparison with the traditional glass-supported metal nanoparticles (MNPs), the introduction of a silicon substrate has been shown to provide an increased surface-enhanced Raman scattering (SERS) effect due to the coupling between the MNPs and the semiconducting silicon substrate. In this work, we further study the fluorescence-enhanced effect of the silicon-supported silver-island (Ag@Si) plasmonic chips. In particular, we investigate their practical application of improving the traditional immunoassay such as the biotin-streptavidin-based protein assay and the protein-/nucleic acid-labeled cell and tissue samples. The protein assay shows a wavelength-dependent enhancement effect of the Ag@Si chip, with an enhancement factor ranging from 1.2 (at 532 nm) to 57.3 (at 800 nm). Moreover, for the protein- and nucleic acid-labeled cell and tissue samples, the Ag@Si chip provides a fluorescence enhancement factor of 3.0–4.1 (at 800 nm) and a significant improvement in the signal/background ratio for the microscopy images. Such a ready accommodation of the fluorescence-enhanced effect for the immunoassay samples

* Corresponding author. College of Physics, Optoelectronics and Energy, Soochow University, Suzhou 215006, PR China.
** Corresponding author. College of Physics, Optoelectronics and Energy, Soochow University, Suzhou 215006, PR China.
*** Corresponding author. Institute of Functional Nano and Soft Materials (FUNSOM), Jiangsu Key Laboratory for Carbon-Based Functional Materials and Devices, Soochow University, Suzhou 215123, PR China.
E-mail addresses: yuanbing@suda.edu.cn (B. Yuan), yaohe@suda.edu.cn (Y. He), yangkai@suda.edu.cn (K. Yang).
[1] These authors contributed equally.

http://dx.doi.org/10.1016/j.aca.2016.11.059

with simple manipulations indicates broad potential for applications of the Ag@Si chip not only in biological studies but also in the clinical field.

1. Introduction

The fluorescence immunoassay is one of the most widely-used methods in protein and nucleic acid detection due to advantages such as high sensitivity, data quantification and rapid analysis, as well as causing minimal damage to samples [1,2]. However, the majority of current fluorescent dyes, especially those that emit wavelengths within the near-infrared range, suffer from low emission intensity which ultimately limits the use of the fluorescence method [3]. To improve the detection sensitivity of the fluorescence assay for practical applications such as early disease detection, the fluorescence signals can be enhanced by metallic nanostructures through surface plasmons of metal, known as "metal-enhanced fluorescence" (MEF) [4–7].

Two approaches have been widely studied for the plasmonic enhancement effect of fluorescence for biosensor and bioassay applications. One approach is based on the particle dispersions of nanoparticles (NPs) such as gold or silver NPs as well as some core-shell nanostructures or nanocomposites [8–10]. Such NPs can work not only as substrates to enhance fluorescence detection, but also, after aptamer functionalization, they are suitable to be directly used as detection probes. The other approach involves using a homogeneous substrate for enhancement [11–14]. Frequently-used examples include a gold- or silver-island film consisting of gold or silver particles deposited on a glass slide substrate [14,15]. Compared with the nanoparticle suspension system, the latter approach shows better reproducibility by overcoming disadvantages such as uncontrollable movement and aggregation of free NPs in the aqueous solution. However, it might also lead to an equal enhancement not only in the signal intensity but also in the background noise during detection and imaging.

The metal-based fluorescence enhancement results from the coupling between metal and fluorophores [16]. Recent studies have shown that compared with the traditional glass-supported metal film, the incorporation of a silicon-based substrate to fabricate a metallic nanohybrid structure shows even higher plasmonic enhancement [17–21]. Very recently, He et al. investigated how silicon substrates facilitate surface-enhanced Raman scattering (SERS) enhancement on a single NP level; this is ascribed to the plasmonic coupling between the adjacent metal NPs as well as between the metal NPs and the semiconducting silicon substrate [22]. However, due to their different physical processes, a plasmonic architecture with high SERS improvement does not necessarily mean a high MEF [4,13]. It has been shown, in both theoretical and experimental studies, that a balance exists between the excitation enhancement and the quenching of fluorescence. It is dependent mainly on the coupling effect, which is determined by the space or distance between the fluorophores and the metal [23–25]. That is, a too-strong coupling (with a distance of less than ~1 nm; this value varies depending on the plasmonic structure) would lead to the quenching of the fluorescence while a too-weak coupling (with a distance larger than a few tens of nanometers) would reduce its enhancement effect; this phenomenon is known as a distance-dependent distribution of the fluorescence enhancement factors [26–29].

Here we further describe the development of the silicon-based plasmonic silver (Ag@Si) chip for fluorescence–enhanced detection. Specifically, we discuss its practical use for improving the signal intensity and signal/background ratio of the traditional protein and DNA assays such as the fluorescence Immunological Histological Chemistry (IHC) and Fluorescence in situ Hybridization (FISH) (Fig. 1). The fluorophores, Dylight 555, CF 647, IR 680 and IR 800, are used in this preliminary study of the plasmonic enhancement effect. The results show that the fluorescence enhancement occurs within the visible to near-infrared wavelength range, in a distance-influenced manner (as demonstrated in Fig. 1). The simple and convenient manipulation, their reliable functionality in conjunction with the traditional and widely-used fluorescence bioassay, and obvious improvement in the signal intensity and the signal/background ratio (especially in the biological window range with a near-infrared wavelength) promise the possibility of using plasmonic Ag@Si chips for practical applications such as medical diagnosis and other biological studies.

2. Experimental section

2.1. Materials

2.1.1. For protein assay

Biotin-labeled N-hydroxysuccinimide (NHS), Troponin and DAPI were purchased from Sigma. Here, Troponin was pre-conjugated with biotin and used as a protein anchor for biotin immobilization on both types of chips. The conjugation of Biotin-Troponin was realized by mixing gently and incubating in a dark room for 2 h at room temperature, followed by purification with columns (illustra NAP-5 Columns; GE Healthcare). Dye-labeled streptavidin was purchased from LI-COR Biosciences. Four types of dyes, including Dylight 555, CF 647, IR 680 and IR 800 (listed in Table 1), were used.

2.1.2. For IHC labeling

Mouse anti-EGFR primary antibody was purchased from Santa Cruz. Dye-conjugated goat-anti-mouse secondary antibody was purchased from Life Technologies. IR 680 and IR 800 dyes were used.

2.1.3. For FISH labeling

NIR-797-isothiocyanate (manufactured by Chemodex, also listed in Table 1) was purchased from AdipoGen Life Sciences. Amino-modified miRNA probes, targeting miRNA29a (positive for human glioma (U87), with the probe sequence as ZTAACCGATTTCA-GATGGTGCTAAAAAAAAAAAX) and miRNA155 (negative for U87, ZACCCCTATCACGATTAGCATTAAAAAAAAAAAAX) segments, were ordered from the Protein and Nucleic Acid Biotechnology Facility at Stanford University. The conjugation of miRNA probes with NIR-797-isothiocyanate dye was carried out by mixing (gently shaking) and incubating overnight in the dark at room temperature, followed by purification with column and dialysis (Slide-A-Lyzer MINI Dialysis Units, 3500 MWCO; Thermo Scientific). Proteinase k, Denhardt's, salmon sperm DNA and yeast tRNA were purchased from Thermo Fisher Scientific. Paraformaldehyde (PFA), sodium dodecyl sulfonate (SDS), dextran sulfate, PBS and SSC buffer were purchased from Sigma-Aldrich.

Breast cancer MDA-MB-468 cells and the tissues of squamous cell carcinoma (SCC) and human glioma (U87), frozen in the

Please cite this article in press as: B. Yuan, et al., Plasmon-enhanced fluorescence imaging with silicon-based silver chips for protein and nucleic acid assay, Analytica Chimica Acta (2016), http://dx.doi.org/10.1016/j.aca.2016.11.059

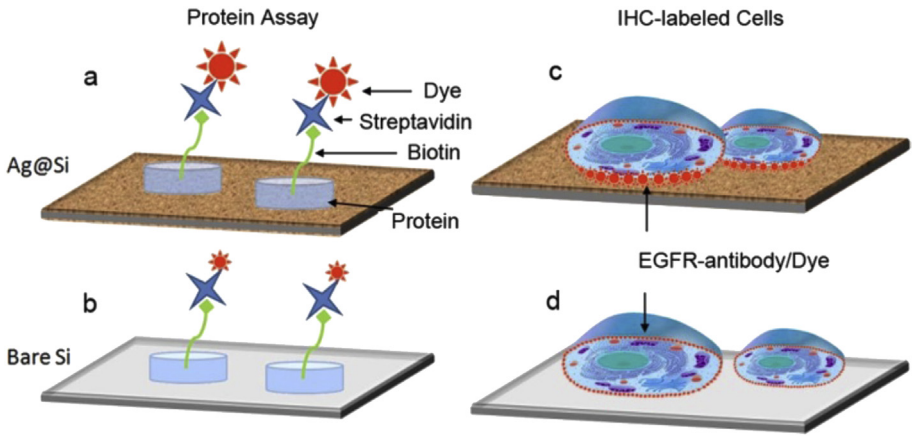

Fig. 1. Schematics showing the Ag@Si enhancement in the protein assay (a, b) and EGFR-labeled cells (c, d). In the comparison between a and b (c and d), a larger star size refers to an enhanced fluorescence intensity.

Table 1
Summary of dyes.

Dye	Abs (max)/nm	Em (max)/nm	Ext. Coeff. (in 1X PBS)/M^{-1} cm^{-1}	Manufacturer
NIR 797	795	817	48,500	Chemodex
IR 800	774	789	240,000	LI-COR
IR 680	676	693	250,000	LI-COR
CF 647	650	665	240,000	Sigma
Dylight 555	555	565	150,000	OriGene

optimal cutting temperature compound (OCT), were received as gifts from Prof. Zhen Chen at the School of Medicine, Stanford University. The cells were cultivated in Leibovit's Medium (Gibco). The tissue was cut into sections with a thickness of 8 μm, transferred onto the amino-modified surface of a cover glass, and temporarily stored in the −80 °C refrigerator for use.

2.1.4. For Ag@Si chip preparation

Hydrofluoric acid (HF, ≥40%), acetone, hydrogenperoxide (H_2O_2, ≥30%), and sulfuric acid (H_2SO_4, 98%) were purchased from Sinopharm Chemical Reagent Co., Ltd. (Shanghai, China). Silver nitrate ($AgNO_3$, ≥99.8%) was purchased from Nanjing Chemical Reagent Co., Ltd. (China). Silicon (100) wafers (phosphate-doped, p-type, 0.01–0.02 Ω sensitivity) were bought from Hefei Kejing Materials Technology Co., Ltd. (Hefei, China). All chemicals were used without additional purification. All solutions were prepared in Milli-Q water (Millipore, 18.2 MΩ cm^{-1}) at room temperature.

2.2. Preparation of the plasmonic Ag@Si chip

A silicon wafer was cleaned with acetone by ultrasonic treatment for 10 min and washed with Milli-Q water three times. Afterward, the silicon wafer was immersed in an oxidant solution containing H_2SO_4 (98%) and H_2O_2 (30%) with a volume ratio of 3:1 for 20 min, and rinsed with Milli-Q water three times to remove organic contaminants. The cleaned silicon wafer was then immersed in a hydrogen fluoride (HF, 5%) aqueous solution for 30 min to achieve a fresh H-terminated silicon wafer covered by Si—H bonds. The H-terminated silicon wafer was then immediately placed into a freshly-prepared reduction solution containing $AgNO_3$ (0.5 mmol L^{-1}) and HF (10%) and was slowly stirred for 60 min at room temperature. AgNPs were readily grown on the surface of the silicon wafer via a reduction reaction, producing an AgNPs-decorated silicon wafer (plasmonic Ag@Si chip). The resulting plasmonic Ag@Si chip was dried with a gentle flow of nitrogen gas and used as plasmon-enhanced fluorescence substrate for the following experiment. Scanning electron microscopy (SEM, Raith Pioneer) and atomic force microscopy (AFM, Asylum Research MFP-3D-SA) characterizations were carried out.

2.3. Microarray printing and assay procedure on Ag@Si and bare Si surface

2 μM biotin-conjugated Troponin in PBS was printed onto the Ag@Si- and bare Si-slide surface using a microarray printing robot (Bio-Rad VersArray Chipwriter) at room temperature [14]. The slides were blocked with 5% FBS (diluted in phosphate buffered saline-Tween 20 (PBST)) before being incubated with 2 nM dye-labeled streptavidin for 1 h in the dark at room temperature. After that, the chips were washed thoroughly with PBST, PBS and finally DI water, dried under air flow, and measured immediately with a scanner. Here, four different types of dyes were used: Dylight 555, CF 647, IR 680 and IR 800.

2.4. Fabrication of the fluorescence IHC- and FISH-labeled samples of cells and tissue sections

The MDA-MB-468 cells were first seeded on the Ag@Si- and bare Si-slide surfaces at a number density of ~80 cells per mm^2 and incubated overnight at 37 °C. After washing with PBS, the cells were EGFR-labeled according to the standard fluorescence IHC protocols. Briefly, the cells were fixed with freshly-made 4% PFA for 10 min, permeated with iced methanol for 10 min, and blocked with 50 mg mL^{-1} BSA for 1 h. The mouse anti-EGFR primary antibody (diluted at 1:1000 in 50 mg mL^{-1} BSA) was added to the cells and incubated for 2 h at room temperature. After removing the extra solution and washing completely with PBS three times, the IR 800 dye-labeled goat-anti-mouse secondary antibody (diluted at 1:1000 in 50 mg mL^{-1} BSA) was added, incubated for another 2 h at room temperature, and washed again. The cells were further

Please cite this article in press as: B. Yuan, et al., Plasmon-enhanced fluorescence imaging with silicon-based silver chips for protein and nucleic acid assay, Analytica Chimica Acta (2016), http://dx.doi.org/10.1016/j.aca.2016.11.059

nucleus-stained with 10 μg mL^{-1} DAPI for 10 min, washed with PBS and DI water, dried under air flow and observed immediately with fluorescence scanner and microscope. The fluorescence IHC cell samples shown in this report were prepared following this procedure, unless otherwise mentioned.

The cells were also stained in solution before seeding on the substrate for reference. Briefly, the cells were trypsinized, washed in the centrifuge (1000 rpm, 2 min) and re-dispersed in PBS. Cell fixing, permeation and blocking were carried out directly in the solution, followed by staining with primary antibody and dye-conjugated secondary antibody. The cells were washed thoroughly before being seeded on the Ag@Si and bare Si surface while incubating at 37 °C overnight. Finally, the cells were stained with DAPI, washed with PBS and DI water and dried for observation.

For the IHC fluorescence labeling of tissue sections, similar steps were followed. Before treatment, the frozen sections of SCC (positive for anti-EGFR protein) and HepG2 (negative for anti-EGFR protein) tissues were removed from the −80 °C refrigerator and incubated for 1 h at 37 °C. Then, the tissue was fixed with iced methanol for 10 min and blocked with 20% FBS (diluted in PBST) for 30 min. The mouse anti-EGFR primary antibody (diluted at 1:1000 in 20% FBS) was added to the cells, incubated overnight at 4 °C, and washed thoroughly. Then, the IR 800 or IR 680 dye-labeled goat anti-mouse secondary antibody (diluted at 1:1000) was added, incubated for another 2 h at room temperature, and washed again. After DAPI staining and washing, the tissues were infiltrated with 20% glycerol, half-covered with Ag@Si plasmonic chips, and observed immediately under the fluorescence scanner and microscope. Observation was performed directly on the cover glass side.

For the DNA labeling of U87 tissue, the standard FISH protocol was employed. Before treatment, the frozen sections of U87 tissue were incubated at 37 °C for 1 h. The operations after that are detailed as follows. (1) For each section, it was first immersed in 200 μL of freshly prepared 4% PFA for 10 min, washed with 1 × PBS three times, then treated with Proteinase k solution (at 5 μg mL^{-1} in 1 × PBS) for 20 min, followed by 3 rounds of PBS washing. All operations were carried out at room temperature. (2) 30 μL of pre-hybridization mixture (30% formamide, 2 × SSC, 1 × Denhardt's, 0.02% SDS, 0.5 mg mL^{-1} salmon sperm DNA, 0.5 mg mL^{-1} yeast tRNA) was added to each section and incubated at 37 °C for 2 h. After removing the excess solution, 30 μL of hybridization mixture (25 nM NIR-797-miRNA Probe, 30% formamide, 2 × SSC, 10% dextran sulfate, 1 × Denhardt's, 0.5 mg mL^{-1} salmon sperm DNA, 0.5 mg mL^{-1} yeast tRNA) was added to each slide and incubated at 37 °C overnight. The sections were covered with parafilms and kept in a humidified chamber to prevent solvent evaporation. (3) After incubation, each section was washed with 2 × SSC at 40.5 °C for 10 min. The washing step was repeated three times for the complete removal of non-specifically adsorbed dye-conjugated probes. The washing was finalized with 2 × SSC for 5 min at room temperature. The samples were also incubated with 5 μg mL^{-1} DAPI for 10 min at room temperature for nucleus staining, followed by PBS washing. Finally, they were infiltrated with 20% glycerol, half-covered with Ag@Si plasmonic chips and then immediately observed.

2.5. Fluorescence characterization with scanner and microscope

A GenePix 4000B microarray scanner and a Li-COR Odyssey infrared imaging system were used to scan the visible- and near-infrared dye-labeled samples, respectively, on different substrates (as detailed in Table S1 in the supporting information). The fluorescence intensities of dyes Dylight 555 and CF 647 were obtained with GenePix through the 532 nm and 635 nm channels, respectively, while the fluorescence intensities from dyes IR 680 and IR 800 were obtained through the 700 nm and 800 nm channels with Li-COR. The fluorescence micrographs were obtained with an EVOS (Life Technologies) cell imaging system, through the IR800, IR680 and DAPI channels respectively (detailed in Table S1). All characterizations were carried out within 2 h of the sample preparation.

2.6. Data analysis

Quantitative analysis of the fluorescence intensity for the microarray fluorescence images was performed with GenePix 6.1. An average value of the fluorescence intensities for each plot was first calculated and then an average of the nine plots and triplicated samples was calculated, representing the signal intensity of the dye. An average value of the background intensities was obtained as well. The enhancement factor for Ag@Si chip over bare Si was defined as the ratio between the fluorescence intensity on Ag@Si (dye intensity minus background intensity) and that on bare Si. The enhancement factor for the IHC-labeled cell samples was calculated in a similar manner, whereby the signal intensity was averaged from at least 70 cells from triply-repeated experiments.

The fluorescence intensity of the IHC- or FISH-labeled tissue samples under specific conditions was averaged from a homogeneous area of at least 2 × 2 mm^2 within the region of the sample. All experiments were repeated at least three times to ensure reproducibility.

3. Results and discussion

3.1. Characterization of the plasmonic Ag@Si chip

The morphology of the Ag@Si chip was investigated using SEM and AFM as shown in Fig. 2. Throughout the whole Ag@Si chip (with dimensions of ~3 cm by 8 cm), the silicon substrate was homogeneously covered by a layer of silver islands with a thickness of approximately 200 nm. In one of our previous papers, we showed that uniform SERS spectra with similar intensity values can be obtained across the area of the sample [13,19].

3.2. Ag@Si enhancement effect on microarray of protein assay

The biotin-streptavidin interaction was employed for the protein assay on both Ag@Si- and bare Si-slide surfaces to demonstrate the fluorescence enhancement effect of the plasmonic Ag@Si chip in comparison with bare Si: different wavelength ranges were used (Fig. 1a and b). Biotin-conjugated Troponin was pre-printed on the two types of slide surface, with nine parallel spots for each sample, and then detected with the dye-conjugated streptavidin. The abundance of the captured protein was reflected by the intensity of the dye's fluorescence. Fig. 3a shows the comparison between Ag@Si- and bare Si-supported fluorescence arrays labeled with four different dyes, including IR 800, IR 680, CF 647 and Dylight 555: their fluorescence intensities were captured through the 800, 700, 635 and 532 nm channels of the scanner, respectively (Table S1 in Supporting Information). It is shown that for the IR 800, IR 680 and CF 647 dyes, the fluorescence on the Ag@Si surface can be clearly observed, while it is hardly distinguishable on the bare Si surface (this is shown with magnified brightness in the inset for reference). However, for the Dylight 555 dye, the fluorescence intensity on bare Si seems comparable to that on a Ag@Si surface. Quantitative analysis of the fluorescence intensity for each sample is shown in Fig. 3b. The calculated average enhanced ratio in fluorescence intensity of the Ag@Si chip over the reference on bare-Si surface was approximately 57.3, 26.9, 5.8 and 1.2-fold, for the IR 800, IR 680, CF 647 and Dylight 555 dyes respectively. These results show that the fluorescence enhancement effect of Ag@Si plasmonic chips is

Please cite this article in press as: B. Yuan, et al., Plasmon-enhanced fluorescence imaging with silicon-based silver chips for protein and nucleic acid assay, Analytica Chimica Acta (2016), http://dx.doi.org/10.1016/j.aca.2016.11.059

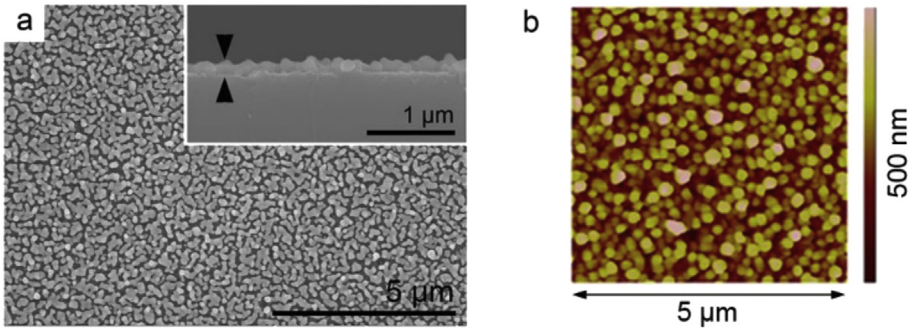

Fig. 2. SEM (a) and AFM (b) graphs of the plasmonic Ag@Si chip. Inset in (a) presents a cross-sectional image showing the thickness of the Ag film (marked by black arrows) deposited on the silicon surface.

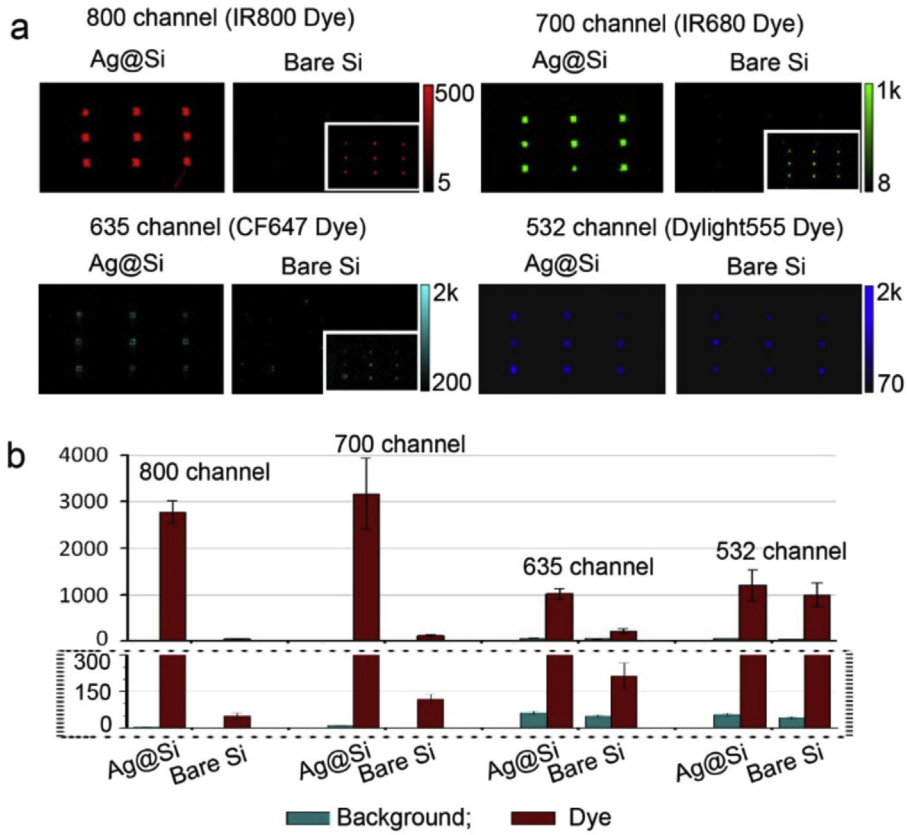

Fig. 3. Microarray of biotin-streptavidin interaction on plasmonic Ag@Si vs. bare Si. Biotin-conjugated Troponin protein was pre-printed and dried on Ag@Si- and bare Si-slides. Streptavidin, conjugated with different types of commercial dyes including IR 800, IR 680, CF 647 and Dylight 555, was immobilized through biotin-streptavidin interactions on the biotin-coated surface. The nine spots for each sample refer to the same meanings. (a) Fluorescence scanner images of microarrays in different channels on Ag@Si vs. Si. Insets show the image with a magnified brightness for clarity. (b) Fluorescence intensity distribution obtained by averaging the integrated fluorescence intensity over the 9 duplicate microarray spots within each channel (while the background intensity was obtained by averaging the space region). Error bars represent the standard deviation (SD) of the mean over the 9 duplicate assay features and triplicated samples. The histogram was regionally magnified (as shown in the dotted rectangle at the bottom). The color-coded fluorescence intensity scale bar is displayed on the right for each channel. (For interpretation of the references to color in this figure legend, the reader is referred to the web version of this article.)

pronouncedly observed for a protein assay, although such an enhancement is dependent on wavelength.

3.3. Ag@Si enhancement effect on IHC-labeled cell and tissue samples

In order to promote this method to a more practical field such as clinical use, fluorescence based IHC-labeled samples of cells (Fig. 1c and d) and tissue sections were fabricated. Fig. 4 shows the comparison of fluorophore-labeled MDA-MB-468 cells seeded on bare Si and Ag@Si chip surfaces, observed under scanner (Fig. 4a) and microscope (Fig. 4c). In addition, bare glass was also used as a substrate for comparison as it is generally used in imaging (Fig. S1 in Supporting Information). The cells were EGFR-targeted with IR 800 dye. Here, only the IR 800 dye was chosen because it is preferred by researchers due to the low indigenous tissue auto-fluorescence in the near-infrared region for biological imaging in comparison with that in the visible range. In fact, scanning analysis

Please cite this article in press as: B. Yuan, et al., Plasmon-enhanced fluorescence imaging with silicon-based silver chips for protein and nucleic acid assay, Analytica Chimica Acta (2016), http://dx.doi.org/10.1016/j.aca.2016.11.059

reveals that the fluorescence intensity of the IHC-labeled cells on a Ag@Si chip looks much brighter than it does on a bare Si wafer. Quantitative fluorescence intensity analysis showed an enhancement ratio of 4.1, which was calculated as the ratio between the signal intensities of the fluorescence-labeled cells on the Ag@Si and bare Si surfaces.

Micrographs of the fluorescence-labeled cells were also shown in IR 800 (for the IR800-labeled EGFR), DAPI (for cell nucleus) and the merged channels (Fig. 4c). For the samples on the Ag@Si and bare Si surfaces, the images for each channel were acquired and shown with identical parameters. It was found that in the IR 800 channel, the fluorescence of the IHC-labeled cells on the Ag@Si chip surface looks much brighter than it does on a bare Si surface. However, for the DAPI channel, little difference can be observed. This indicates that the Ag@Si plasmonic substrate can significantly enhance the fluorescence signal of the IHC-labeled cells at the IR 800 wavelength, but is less effective at the DAPI range. Quantitative analysis can be obtained in the form of a signal/background (S/B) ratio for each image; these were calculated to be 1.3 and 2.2 for the bare Si and Ag@Si chips, respectively (in the IR 800 channel). Moreover, to further confirm that such an improvement effect cannot be achieved through solely prolonging the exposure time under microscope, the sample on bare Si was also captured with a longer time from 1 s to 1.5 and 2.5 s. In these cases, the S/B ratio was only increased to ~1.5 due to the simultaneously increased background noise.

The Ag@Si enhancement measurement was also performed on the fluorescence IHC-labeled tissue sections. Fig. 5 shows the schematic of the sandwiched structure, as well as optical morphology and fluorescence images, under scanner and microscope, of IHC-labeled SCC tissue sections with and without Ag@Si chip covering. Scanner-obtained images of representative samples are shown in Fig. 5d, and quantitative analysis of the average fluorescence intensity for each type of sample region is presented

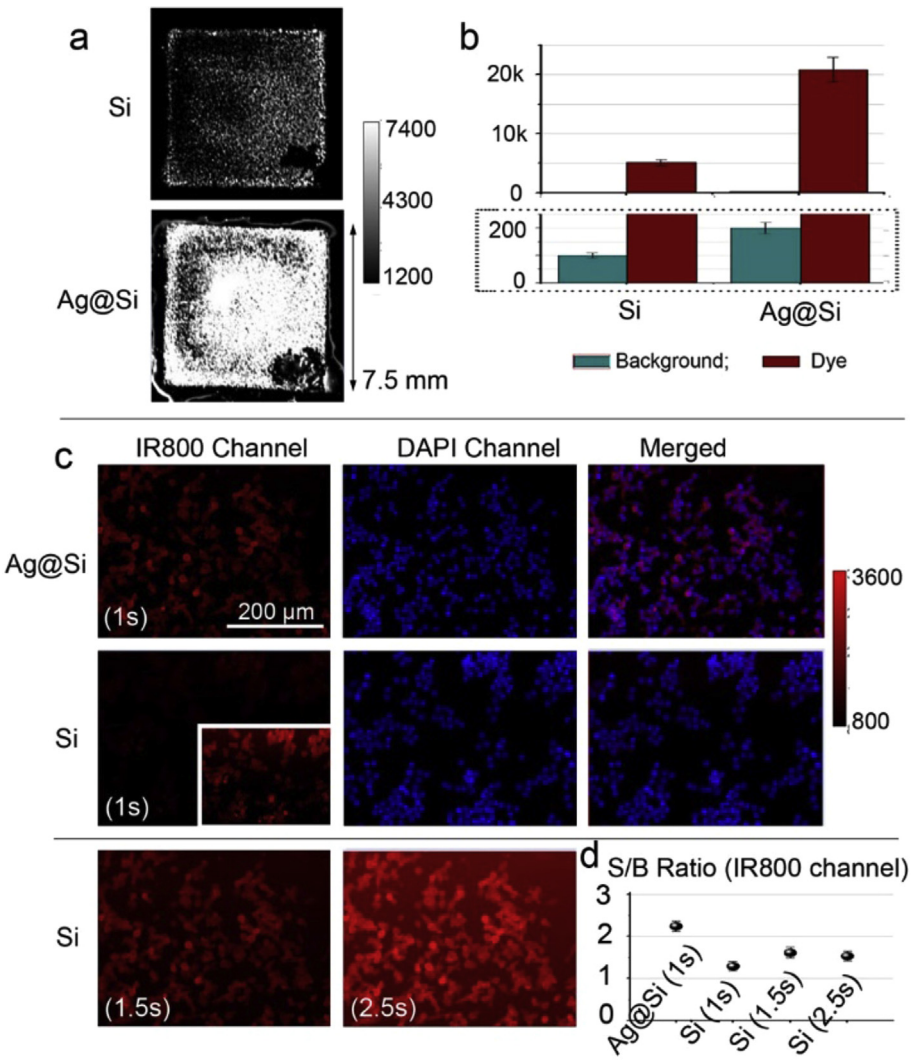

Fig. 4. Fluorescence IHC-labeled breast cancer MDA-MB-468 cells on bare Si wafer vs. Ag@Si chip surface. The cells were modified with mouse anti-EGFR primary antibody followed by IR 800 dye-labeled goat anti-mouse secondary antibody, and finally stained with DAPI. (a) Scanner images in 800 nm channel for the cells on bare Si or Ag@Si surface. The cells were confined in a 7.5 × 7.5 mm^2 well while seeding on the slide surface followed by fixing and staining in situ. (b) Fluorescence intensity distribution of the cells and background obtained from (a). Error bars represent the SD of the mean over at least 70 points in the image. The histogram was regionally magnified (as shown in the dotted rectangle at the bottom) to shown the intensity of the background on each substrate. (c) Corresponding microscopy images of the cells in both IR 800 and DAPI channels, and the merged image. (c)-bottom, cells on Si imaged with a prolonged exposure time of 1.5 or 2.5 s in IR 800 channel. The color-coded fluorescence intensity scale bar is displayed on the right for the IR 800 channel. (d) Signal/background (S/B) ratio distribution in IR800 channel obtained from (c). The intensity of signal and background in each condition was averaged from at least 30 cells/points in the image. Aggregate sizes were measured over a 2.0 mm^2 area for each line array. (For interpretation of the references to color in this figure legend, the reader is referred to the web version of this article.)

Please cite this article in press as: B. Yuan, et al., Plasmon-enhanced fluorescence imaging with silicon-based silver chips for protein and nucleic acid assay, Analytica Chimica Acta (2016), http://dx.doi.org/10.1016/j.aca.2016.11.059

in Fig. 5e. It can be observed that the fluorescence intensity of the regions under a Ag@Si chip is much higher than that without Ag@Si coverage. An enhancement factor of 3.0 was obtained; this represents the ratio between the fluorescence intensities of the regions with and without Ag@Si coverage. A fluorescence enhancement effect was also observed by the micrographs under microscope (Fig. 5f). In the IR 800 channel, the image appears to be much brighter under the Ag@Si chip compared to that without Ag@Si coverage, although they were observed under identical conditions. In comparison, in the DAPI channel, the contrast in fluorescence intensity for samples with and without Ag@Si coverage is somewhat less obvious. The samples labeled with IR 680 dye show similar results and an enhancement ratio of ~3.3 was obtained (Fig. S2, Supporting Information).

In one of the control experiments, we pre-seeded the cells on a cover glass, IHC-labeled them with dyes and partly covered with Ag@Si chips. A similar enhancement factor was obtained at the same wavelength in comparison with those pre-seeded on a chip surface. Moreover, we also IHC-labeled the suspended cells in solution, and then seeded them on the Ag@Si chip and bare-Si surface. Again, a similar enhancement factor was obtained. This result confirms the reproducibility of the enhancement effect of the Ag@Si chips.

3.4. Ag@Si enhancement effect on FISH tissue samples

FISH has been widely used for the detection of specific DNA sequences in both intact cells and isolated chromosomes [30,31]. By labeling and visualizing specific DNA sequences with fluorochromes or even discriminating different targets with multiple fluorophores simultaneously, FISH is now being applied in an increasing number of molecular diagnostic areas, including karyotype analysis, gene mapping, disease diagnosis, and therapeutic targeting. Therefore, improving the fluorescence intensity, especially the S/B ratio of a FISH test, plays a key role in practical applications. In our study, we designed a model experiment to label the miRNA-29a sequence in U87 tissue, and investigated the enhancement effect of the Ag@Si plasmonic chips on the dye-labeled tissue. Meanwhile, a negative (to the anti-EGFR protein) probe was taken for reference, to confirm the targeted labeling of the specific miRNA sequence in U87 cells.

Fig. 6 shows the FISH-labeled U87 tissues with and without

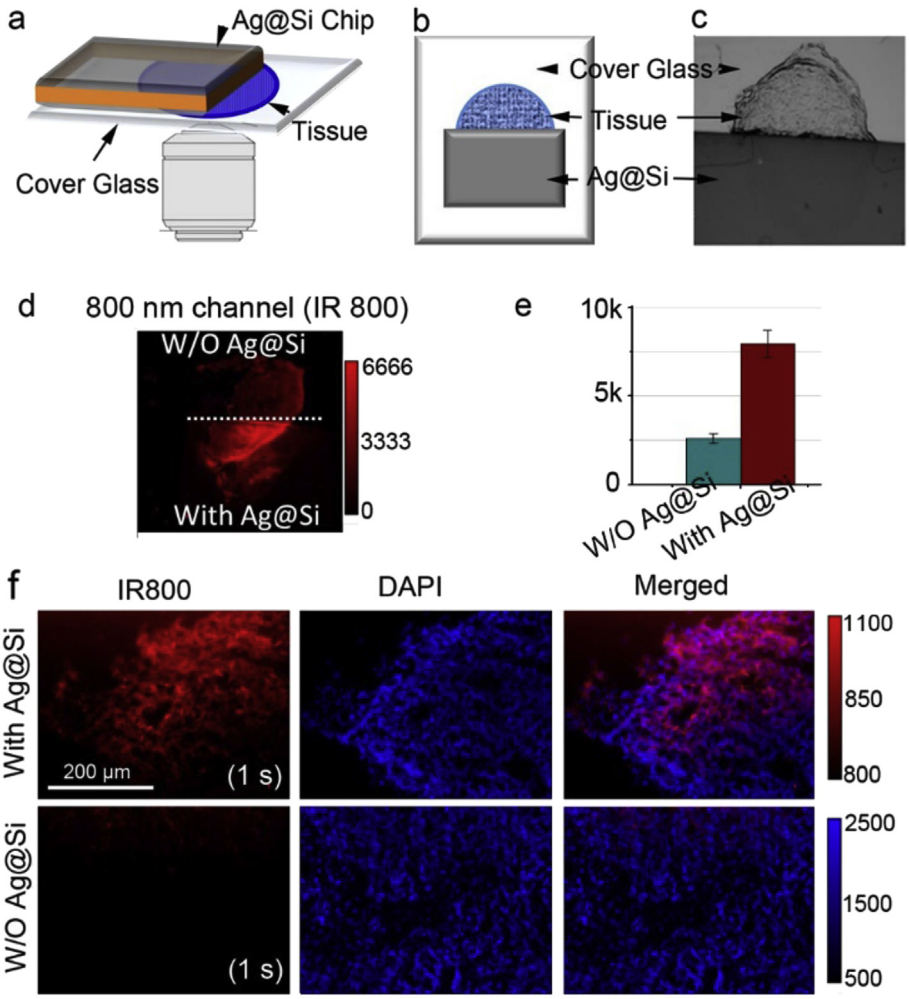

Fig. 5. Fluorescence-based IHC-labeled SCC tissues with vs. without plasmonic Ag@Si enhancement. The tissues were modified with mouse anti-EGFR primary antibody followed by IR 800 dye-labeled goat anti-mouse secondary antibody, then with DAPI, and finally half-covered with Ag@Si chips. (a) Schematic view of the fluorescent assay for tissue with/without Ag@Si coverage. (b) Schematic rendition and (c) bright field images of the sample from a top view. (d) Scanner images of the tissues obtained in 800 nm channel. (e) Fluorescence intensity distribution, which was acquired by averaging the fluorescence intensities of the corresponding areas in (d). Error bars were based on the SD of three parallel samples. (f) Counterpart microscopy images of the SCC tissue with vs. without Ag@Si coverage in different channels. The color-coded fluorescence intensity scale bars are displayed on the right for each channel. (For interpretation of the references to color in this figure legend, the reader is referred to the web version of this article.)

Please cite this article in press as: B. Yuan, et al., Plasmon-enhanced fluorescence imaging with silicon-based silver chips for protein and nucleic acid assay, Analytica Chimica Acta (2016), http://dx.doi.org/10.1016/j.aca.2016.11.059

Ag@Si enhancement under scanner and microscope observations. In Fig. 6a, the miRNA-29a-labeled tissue exhibits an obvious fluorescence signal when analyzed with the NIR-797 probe, while under the same conditions, fluorescence of the negative control sample was hardly distinguishable, unless a magnified brightness was applied (Fig. 6a-right). The ratio of fluorescence intensity between these two samples was 5.7 (without Ag@Si coverage) or 9.4 (with Ag@Si coverage). Considering that the fluorescence signal from the negative control sample is due to the non-specific adsorption of fluorescent probes in the tissue, such a high ratio indicates the targeted labeling of the specific miRNA sequence within the positive sample.

Moreover, for the FISH-labeled tissue, evident contrast in fluorescence intensity occurs between the regions with and without Ag@Si coverage, and an enhancement ratio of 3.2 was obtained. Fig. 6c shows the comparison of fluorescence micrographs between representative regions with and without Ag@Si coverage, which confirms the enhancement effect of the plasmonic chip especially in the IR800 channel. The S/B ratio of the image was improved from 1.1 to 1.8, which cannot be acquired through solely prolonging the exposure time (Fig. 6d).

4. Discussion

From the protein, cell and tissue experiments, it was shown that the Ag@Si plasmonic chip produces a significant enhancement

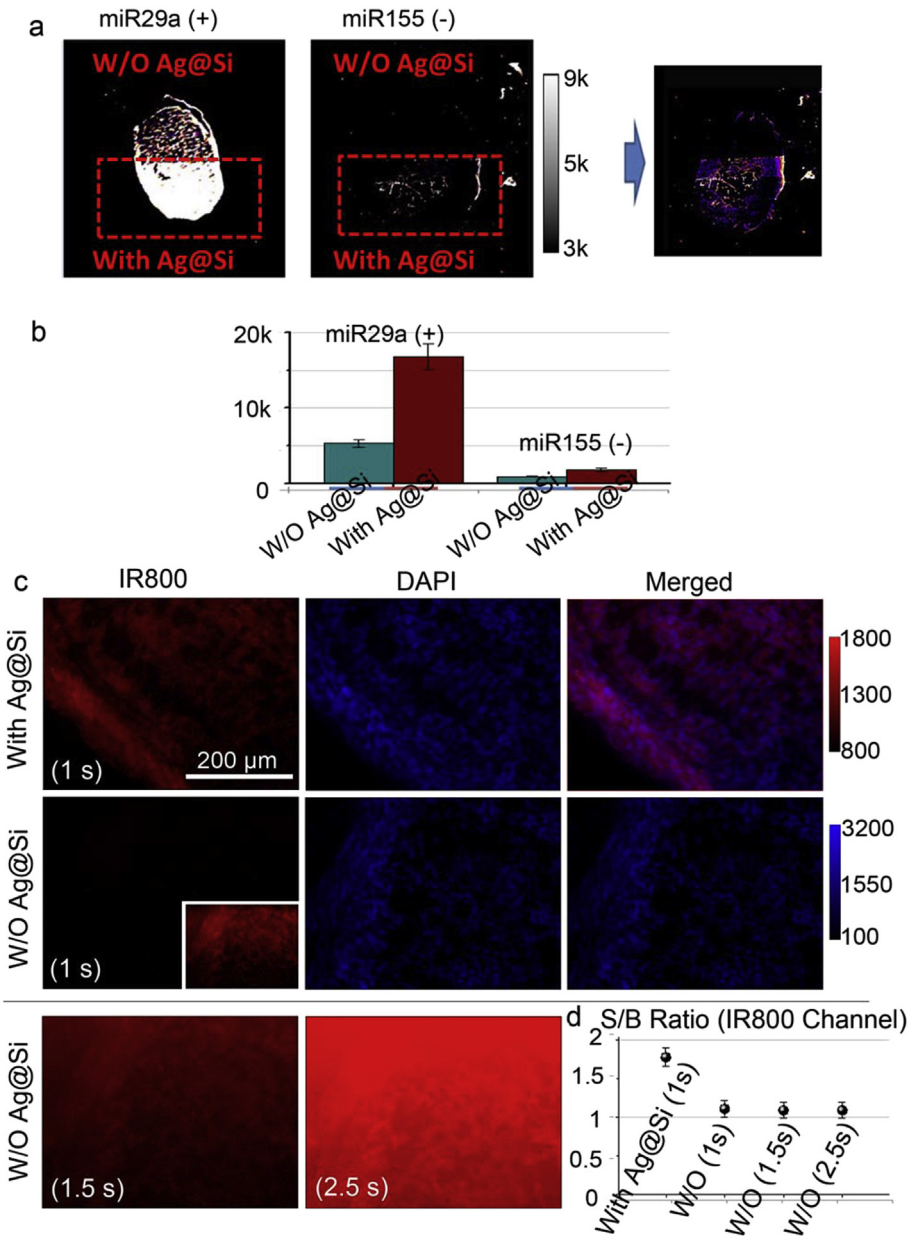

Fig. 6. FISH-labeled U87 tissues, supported on cover glasses and half-covered with Ag@Si chips. The tissue was hybridized with NIR-797-conjugated miRNA29a (positive for U87) and miRNA155 (negative for U87) probes, followed by DAPI staining. (a) Scanner images for both miR29a (+) and miR155 (−) labeled tissues, with and without Ag@Si coverage, acquired in 800 nm channel. The negative control sample was shown with an increased brightness (right) for clarity. (b) Fluorescence intensity distribution of the different regions obtained from (a). (c) Corresponding microscope images for the miR29a labeled tissue with/without Ag@Si coverage, obtained from the IR800 and DAPI channels. Inset shows the image with a magnified brightness for reference. (c)-bottom, the sample without Ag@Si coverage exposed in IR800 channel with a prolonged time of 1.5 or 2.5 s. (d) Distribution of the signal/background ratio in IR800 channel for the images in (c). Error bars in (b) and (d) were based on the SD of three parallel samples.

Please cite this article in press as: B. Yuan, et al., Plasmon-enhanced fluorescence imaging with silicon-based silver chips for protein and nucleic acid assay, Analytica Chimica Acta (2016), http://dx.doi.org/10.1016/j.aca.2016.11.059

effect in fluorescence intensity and ultimately an improvement in S/B ratio for microscopy imaging. Moreover, such an enhancement shows a better effect in the near-infrared wavelength range than it does in the visible range, and is therefore more suitable for biological imaging due to lower tissue noise in this range.

It has been clarified that the fluorescence enhancement effect is greatly determined by the distance between the plasmonic surface and the fluorophores [26,27,29]. A greater distance leads to the reduction of the coupling interaction between the chip surface and the fluorophores and ultimately a much lower plasmonic enhancement. Therefore, in practical applications, the distance between the cell/tissue samples and the plasmonic chips is crucial for a better and more reproducible enhancement effect. During our experiments, the cell samples are preferred to be seeded on the Ag@Si chip surface for signal enhancement. On the other hand, for the samples which have traditionally been supported on a glass surface in clinical use, the covered Ag@Si chip needs to be pressed slightly until the excess glycerol is extruded from between the chip-and-tissue surface.

One of the major purposes of this work is to extend the application of Ag@Si chips for fluorescence enhancement from the laboratory to the clinic. In addition to the enhancement in the microarrays of protein assay (Fig. 1a and b), the Ag@Si chips also show notable improvement for the fluorescence-labeled cell and tissue samples by simply covering the samples with the chips. Our results demonstrated that although only the fluorophores (targeted on the membrane of cells/tissues) adjacent to the chip surface can be enhanced via the plasmonic coupling effect (as shown in Fig. 1c), the whole cell/tissue samples show an obvious enhancement (with an enhancement factor of 3.0 and 4.1 at wavelengths of 700 and 800 nm, respectively) and a significant improvement in S/B ratio.

In the control experiments, we found that a higher dye concentration during IHC-/FISH-labeling of the samples, i.e. a higher fluorescence intensity, further promoted the enhancement factor of the Ag@Si chip. Based on this, it is assumed that the fluorescence-enhanced effect of the plasmonic chip on dyes is higher than that on the background of a sample. This might be the reason why an improvement in S/B ratio can be acquired by Ag@Si chip enhancement, in contrast to the influence from solely prolonging the exposure time during observation, whereby the S/B ratio remains unchanged (Figs. 4d and 6d).

5. Conclusions

In this work, a type of Ag@Si chips, which was fabricated via depositing silver film on the silicon wafer surface, was used as a plasmonic substrate for the determination of pharmaceutical substances and cell/tissue applications, based on the fluorescence enhancement and S/B ratio improvement effects of them.

Our results demonstrate the viable integration of the Ag@Si plasmonic chip into traditional fluorescence-based bioassays. It can also be used simultaneously with other signal-magnification methods, such as the typically-used Tyramide Signal Amplification (TSA) technology, for further enhancement. Therefore, it promises a broad range of applications in biological studies, medical diagnostics, and many other fields. Furthermore, it has been shown that the MEF effect is influenced and can be controlled by regulating many parameters of the NPs such as the size, anisotropism and angle, etc. Finally, the plasmon resonance wavelength of the particle structures can be tuned to match the spectral absorption of certain fluorophores, which promises the possibility of further improving the enhancement efficiency of Ag@Si chips for specialized enhancement purposes [4].

Acknowledgement

This work was financially supported by the National Science Foundation of China (Nos. 91427302, 21422404, 21374074, U1532108 and 11474155).

Appendix A. Supplementary data

Supplementary data related to this article can be found at http://dx.doi.org/10.1016/j.aca.2016.11.059.

References

[1] D.A. Giljohann, C.A. Mirkin, Drivers of biodiagnostic development, Nature 462 (2009) 461–464.
[2] W. Deng, F. Xie, H.T.M.C.M. Baltar, E.M. Goldys, Metal-enhanced fluorescence in the life sciences: here, now and beyond, Phys. Chem. Chem. Phys. 15 (2013) 15695–15708.
[3] D. Darvill, A. Centeno, F. Xie, Plasmonic fluorescence enhancement by metal nanostructures: shaping the future of bionanotechnology, Phys. Chem. Chem. Phys. 15 (2013) 15709–15726.
[4] E. Petryayeva, U.J. Krull, Localized surface plasmon resonance: nanostructures, bioassays and biosensing-A review, Anal. Chim. Acta 706 (2011) 8–24.
[5] J. Yao, M. Yang, Y.X. Duan, Chemistry, biology, and medicine of fluorescent nanomaterials and related systems: new insights into biosensing, bioimaging, genomics, diagnostics, and therapy, Chem. Rev. 114 (2014) 6130–6178.
[6] A. Klinkova, R.M. Choueiri, E. Kumacheva, Self-assembled plasmonic nanostructures, Chem. Soc. Rev. 43 (2014) 3976–3991.
[7] H. Jans, Q. Huo, Gold nanoparticle-enabled biological and chemical detection and analysis, Chem. Soc. Rev. 41 (2012) 2849–2866.
[8] C. Ayala-Orozco, J.G. Liu, M.W. Knight, Y. Wang, J.K. Day, P. Nordlander, N.J. Halas, Fluorescence enhancement of molecules inside a gold nanomatryoshka, Nano Lett. 14 (2014) 2926–2933.
[9] S. Khatua, P.M.R. Paulo, H. Yuan, A. Gupta, P. Zijlstra, M. Orrit, Resonant plasmonic enhancement of single-molecule fluorescence by individual gold nanorods, ACS Nano 8 (2014) 4440–4449.
[10] H. Yuan, S. Khatua, P. Zijlstra, M. Yorulmaz, M. Orrit, Thousand-fold enhancement of single-molecule fluorescence near a single gold nanorod, Angew. Chem. Int. Ed. Engl. 52 (2013) 1217–1221.
[11] H. Li, W. Qiang, H. Hu, W. Li, D. Xu, Metal-enhanced fluorescent detection for protein microarrays based on a silver plasmonic substrate, Analyst 139 (2014) 1653–1660.
[12] Y. Shen, T. He, W. Wang, Y. Zhan, X. Hu, B. Yuan, X. Zhou, Fluorescence enhancement on silver nanoplates at the single- and sub-nanoparticle level, Nanoscale 7 (2015) 20132–20141.
[13] L. Zhou, F. Ding, H. Chen, W. Ding, W. Zhang, S.Y. Chou, Enhancement of immunoassay's fluorescence and detection sensitivity using three-dimensional plasmonic nano-antenna-dots array, Anal. Chem. 84 (2012) 4489–4495.
[14] B. Zhang, R.B. Kumar, H. Dai, B.J. Feldman, A plasmonic chip for biomarker discovery and diagnosis of type 1 diabetes, Nat. Med. 20 (2014) 948–953.
[15] M.G. Sreenivasan, S. Malik, S. Thigulla, B.R. Mehta, Dependence of plasmonic properties of silver island films on nanoparticle size and substrate coverage, J. Nanomater (2013) 1–8.
[16] E. Petryayeva, U.J. Krull, Localized surface plasmon resonance: nanostructures, bioassays and biosensing - a review, Anal. Chim. Acta 706 (2011) 8–24.
[17] H. Wang, X. Jiang, S.-T. Lee, Y. He, Silicon nanohybrid-based surface-enhanced Raman scattering sensors, Small 10 (2014) 4455–4468.
[18] E.J. Guidelli, A.P. Ramos, O. Baffa, Enhancing and quenching luminescence with gold nanoparticle films: the influence of substrate on the luminescent properties, Nanotechnology 27 (2016) 015503.
[19] Z.Y. Jiang, X.X. Jiang, S. Su, X.P. Wei, S.T. Lee, Y. He, Silicon-based reproducible and active surface-enhanced Raman scattering substrates for sensitive, specific, and multiplex DNA detection, Appl. Phys. Lett. 100 (2012) 203104.
[20] X. Jiang, Z. Jiang, T. Xu, S. Su, Y. Zhong, F. Peng, Y. Su, Y. He, Surface-enhanced raman scattering-based sensing in vitro: facile and label-free detection of apoptotic cells at the single-cell level, Anal. Chem. 85 (2013) 2809–2816.
[21] H. Wang, X. Jiang, X. Wang, X. Wei, Y. Zhu, B. Sun, Y. Su, S. He, Y. He, Hairpin dna-assisted silicon/silver-based surface-enhanced raman scattering sensing platform for ultrahighly sensitive and specific discrimination of deafness mutations in a real system, Anal. Chem. 86 (2014) 7368–7376.
[22] S.-Y. Wang, X.-X. Jiang, T.-T. Xu, X.-P. Wei, S.-T. Lee, Y. He, Reactive ion etching-assisted surface-enhanced Raman scattering measurements on the single nanoparticle level, Appl. Phys. Lett. 104 (2014) 243104.
[23] P. Anger, P. Bharadwaj, L. Novotny, Enhancement and quenching of single-molecule fluorescence, Phys. Rev. Lett. 96 (2006) 113002.
[24] J. Azoulay, A. Debarre, A. Richard, P. Tchenio, Quenching and enhancement of single-molecule fluorescence under metallic and dielectric tips, Europhys. Lett. 51 (2000) 374–380.
[25] D.A. Weitz, S. Garoff, J.I. Gersten, A. Nitzan, The enhancement of Raman scattering, resonance Raman scattering, and fluorescence from molecules

adsorbed on a rough silver surface, J. Chem. Phys. 78 (1983) 5324–5338.
[26] A.I. Dragan, E.S. Bishop, J.R. Casas-Finet, R.J. Strouse, J. McGivney, M.A. Schenerman, C.D. Geddes, Distance dependence of metal-enhanced fluorescence, Plasmonics 7 (2012) 739–744.
[27] H. Mishra, B.L. Mali, J. Karolin, A.I. Dragan, C.D. Geddes, Experimental and theoretical study of the distance dependence of metal-enhanced fluorescence, phosphorescence and delayed fluorescence in a single system, Phys. Chem. Chem. Phys. 15 (2013) 19538–19544.
[28] B. Fu, J.D. Flynn, B.P. Isaacoff, D.J. Rowland, J.S. Biteen, Experimental and theoretical study of the distance dependence of metal-enhanced fluorescence, phosphorescence and delayed fluorescence in a single system, J. Phys. Chem. C 119 (2015) 19350–19358.
[29] D. Cheng, Q.-H. Xu, Separation distance dependent fluorescence enhancement of fluorescein isothiocyanate by silver nanoparticles, Chem. Commun. (2007) 248–250.
[30] C.M. Price, Fluorescence in-situ hybridization, Blood Rev. 7 (1993) 127–134.
[31] J.M.S. Bartlett, Fluorescence in situ hybridization, Method. Mol. Med. 97 (2004) 77–87.

Please cite this article in press as: B. Yuan, et al., Plasmon-enhanced fluorescence imaging with silicon-based silver chips for protein and nucleic acid assay, Analytica Chimica Acta (2016), http://dx.doi.org/10.1016/j.aca.2016.11.059